ARTICLES
PUBLISHED ONLINE: 13 MARCH 2011 | DOI: 10.1038/NCHEM.1006
nature chemistry

A two-dimensional phase of TiO_2 with a reduced bandgap

Junguang Tao, Tim Luttrell and Matthias Batzill*

Titanium dioxide is the prototypical transition metal oxide photocatalyst. However, the larger than 3 eV bandgap of common bulk phases of TiO_2 limits its light absorption to UV light, making it inefficient for solar energy conversion. Attempts at increasing visible light activity by narrowing the bandgap of TiO_2 through doping have proven difficult, because of defect-induced charge trapping and recombination sites of photo-excited charge carriers. Here, we report the existence of a dopant-free, pure TiO_2 phase with a narrow bandgap. This new pure TiO_2 phase forms on the surface of rutile TiO_2(011) by oxidation of bulk titanium interstitials. We measure a bandgap of only ~2.1 eV for this new phase, matching it closely with the energy of visible light.

Since the discovery of water splitting over TiO_2 by Fujishima and Honda almost 40 years ago[1], the photocatalytic properties of TiO_2 have been widely studied. In addition to the ultimate goal of producing chemical fuels using photocatalysis, the use of TiO_2 in practical applications such as air and water purification and self-cleaning/sterilizing surfaces has been investigated[2]. However, the larger than 3 eV bandgap of the common TiO_2 polymorphs, rutile and anatase, limits their photoactivity to the UV region of the spectrum, making TiO_2 an inefficient material for solar light applications. In recent decades, large efforts have been expended in an attempt to reduce the bandgap of TiO_2 so as to harvest a larger portion of sunlight. Different approaches for narrowing the bandgap have been pursued to increase visible light absorption. The most common method is to dope TiO_2 with impurities[3]. Although recent successes have been reported in achieving visible light activity by using anion dopants such as nitrogen or carbon[4,5], the dopant-induced defects in the TiO_2 lattice have a degrading effect on photochemical activity, largely by the introduction of charge carrier trapping and recombination sites[3]. These degrading effects negate the increase in visible light absorption and cause a reduced photoactivity in the doped TiO_2. Clearly, a dopant-free, pure TiO_2 phase with a bandgap that matches the visible light energy would be ideal. Recently, it was suggested that high-pressure TiO_2 phases with such properties might exist[6,7]. Unfortunately, these phases are not stable at atmospheric pressure, and are therefore not useful for photocatalysis. The surface phases of pure TiO_2 with reduced bandgaps, on the other hand, may be stable under ambient conditions[8,9]. In this Article, we report the discovery of a new two-dimensional TiO_2 phase that has a markedly reduced bandgap compared to common bulk phases of TiO_2. This low-dimensional phase of TiO_2 is formed at the rutile TiO_2(011) surface, so a material consisting entirely of TiO_2 may be synthesized. We measured the bandgap of this new phase to be ~2.1 eV, which is close to perfect for visible light absorption.

Results and discussion

Formation of TiO_2 (011) surface phases. TiO_2(011) single crystals were prepared in vacuum by repeated ion sputtering and vacuum annealing to ~650 °C. This cleaning procedure results in slightly reduced crystals, evident from the formation of colour centres, which give the crystal a bluish hue[10]. The (011) crystallographic surface orientation of rutile TiO_2 exhibits a (2×1) reconstruction, the structure of which has been resolved recently[11,12]. Scanning tunnelling microscopy (STM) images of this surface are shown in Fig. 1a,b. It is well established that re-oxidation of titanium interstitials occurs if slightly vacuum-reduced TiO_2 samples are annealed in a low-pressure O_2 atmosphere[13,14]. In this process, the mobile bulk titanium interstitials diffuse to the surface, where they react with oxygen adsorbed at the surface from the gas phase. This phenomenon has been thoroughly studied on the more frequently investigated rutile TiO_2(110) surface. On the (110) surface, the re-oxidation process results in a layer-by-layer growth of TiO_2 via an intermediate titania sub-oxide phase[15,16]. If the same procedure is applied to the (011) crystal orientation, we also observe a re-oxidation of titanium interstitials and the formation of ordered TiO_2 islands. However, the high-resolution STM images shown in Fig. 1c,d, illustrate that the structure of these islands is different from the original TiO_2(011)–(2×1) surface or a (1×1) bulk truncation. Although the surface periodicity of the new surface structure can also be ascribed as a (2×1) surface unit cell, the structure appears distinctively different in STM images. In particular, on the atomic scale, the new surface phase is less corrugated along the long axis of the surface unit cell than the 'original' surface structure, although it has a similar corrugation along the short axis of the unit cell. The corrugation measured in the STM images is shown as the line scan in Fig. 1e. Importantly, the bright protrusions observed in the STM images are arranged in a (distorted) hexagonal arrangement, thus exhibiting a symmetry different from the rectangular (011) bulk planes of the rutile substrate. This new surface phase is metastable; that is, it appears to have a local energy minimum, but this is not the thermodynamically lowest energy structure. Consequently, annealing in vacuum results in re-formation of the original (2×1) surface reconstruction, which is the lowest energy configuration. However, the new metastable phase is quite thermally stable up to 800 K, indicating significant barriers for re-formation of the original surface structure.

By low-pressure oxygen annealing of the samples used in this study, 10–60% of the surface is usually covered with this new structure. The incomplete transformation of the surface is likely caused by the limited amount of titanium interstitials available for re-oxidation. Additional studies of homo-epitaxial growth of TiO_2 by physical

Department of Physics, University of South Florida, Tampa, Florida 33620, USA. *e-mail: mbatzill@usf.edu

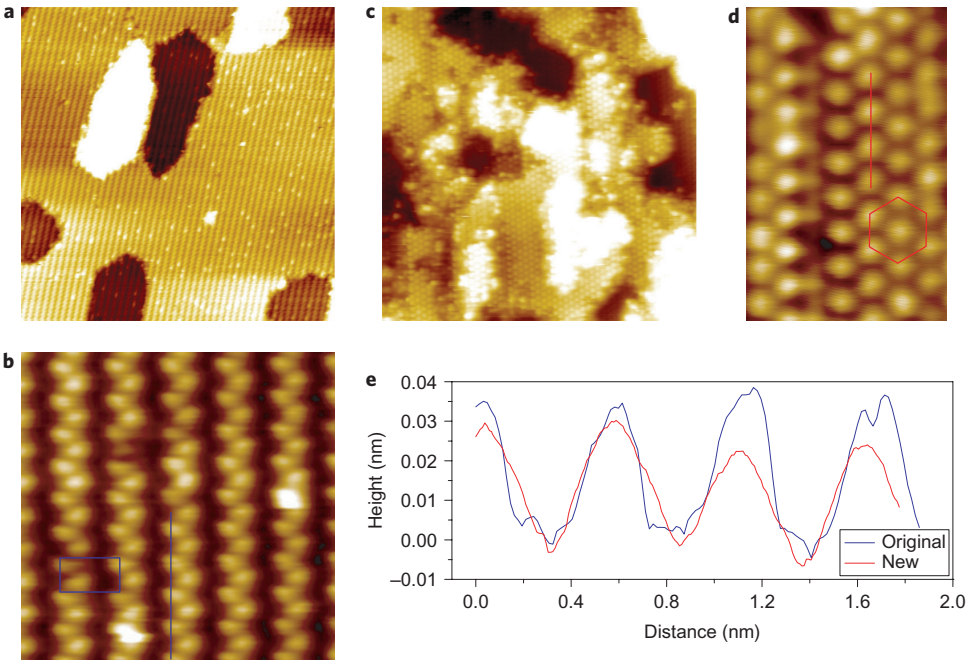

Figure 1 | Atomic-resolution STM images of the rutile TiO_2(011) surface. a,**b**, The (2 × 1) reconstructed surface. **c**,**d**, The new TiO_2 phase formed after annealing in a 1×10^{-6} torr O_2 atmosphere. Image size (**a**,**c**), 50 × 50 nm^2. The surface unit cell for the rectangular (2 × 1) reconstruction is indicated in **b** and the quasi-hexagonal symmetry of the new TiO_2 phase is shown in **d**. A line defect in the new TiO_2 phase can also be seen in **d**. This defect is an anti-phase boundary due to the registry of the new phase with the TiO_2(011) substrate. **e**, Line profiles indicating the atomic corrugation along the indicated lines in **b** and **d**.

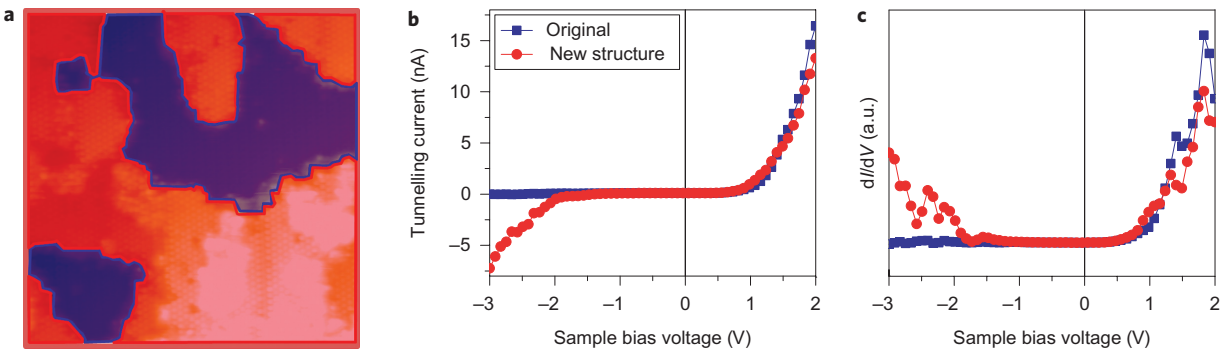

Figure 2 | Scanning tunnelling spectroscopy (STS) measurements. a, Sample prepared so that both 'new' and 'original' phases are present simultaneously at the surface. The original (2 × 1) reconstructed surface is shown in blue, and the new TiO_2 phase in red. **b**, *I*-*V* spectra taken in the two surface areas (blue, original surface; red, new structure). **c**, Numerically differentiated d*I*/d*V* curves. The new surface phase exhibits additional electronic states at negative voltages (filled states). The empty states (positive bias voltage) are shifted slightly towards the Fermi level for the new TiO_2 phase. Thus, although STS cannot provide absolute values for the bandgap due to the strong electric field between the measuring probe and the sample, comparison of the STS spectra on the two surface structures unambiguously identifies a bandgap narrowing for the 'new' structure relative to the 'original' structure.

vapour deposition of titanium in a 10^{-6} torr O_2 background at ~600 K confirmed that more of the surface can be covered by this new structure. From STM images, we found a maximum of 80% of the surface exhibiting the new structure upon homo-epitaxial growth (see Supplementary Information). Furthermore, these homo-epitaxial growth studies confirmed that TiO_2 growth at the surface causes the formation of the new structure, thus excluding the possibility of impurity segregation from the bulk as has been previously suggested[17]. Investigation by Auger electron spectroscopy (AES) also suggested pure TiO_2 to comprise this new metastable surface phase (see Supplementary Information).

Bandgap. To investigate the bandgap of this new phase we performed scanning tunnelling spectroscopy (STS) and ultraviolet photoemission spectroscopy (UPS). STS allows the differentiation of the local electronic structure; this is particularly important for this non-uniform surface, which exhibits two different structures. Figure 2b presents spectra obtained for the original TiO_2(011)–(2 × 1) surface structure and the new TiO_2 phase. When STS is carried out on semiconducting surfaces, the applied voltages cause a band bending, and, as a result, the measured 'bandgap' is not a reliable measure of the position of the electronic states[18]. Nevertheless, a comparison of the STS spectra of the two phases shows that the new phase exhibits filled electronic states that are in the bandgap region of rutile TiO_2. Also, the empty states exhibit a weak variation between the two surfaces, with the conduction band minimum slightly shifted towards the Fermi level (E_F) for the new phase. Therefore, these spectra unambiguously demonstrate that the new TiO_2 phase has a

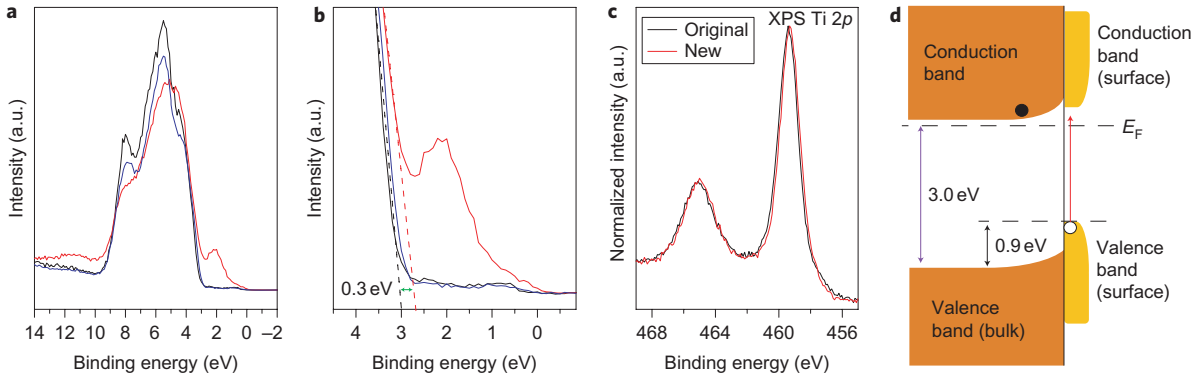

Figure 3 | Comparison of TiO_2 phases by photoemission spectroscopy. a,b, UPS spectra taken with a photon energy of 80 eV: full valence band, with 0 eV binding energy corresponding to the Fermi level (**a**); zoomed in view of the low binding energy region (**b**). The black curve corresponds to the photoemission spectrum for the original (2 × 1) reconstructed surface. The red curve was acquired after low-pressure oxidation and (partial) formation of a new TiO_2 phase. The blue line indicates a photoemission spectrum that has been taken after annealing the sample to ~600 °C in vacuum and re-formation of the original (2 × 1) surface structure. For the new TiO_2 phase a new state is formed with a peak at a binding energy of 2.1 eV. Also, a ~0.3 eV upward shift of the bulk bands is observed due to band bending at the surface. **c**, XPS spectra of the Ti 2*p* core level before (black line) and after (red line) oxygen treatment. No indication for formation of a Ti^{3+} sub-oxide can be detected, and the line shape barely changes with the oxidation procedure, apart from a slight upward shift of the spectrum after oxidation induced by band bending. **d**, Band diagram, deduced from UPS and STS, together with an indication of a proposed electron–hole separation of photo-excited electron–hole pairs at this surface. The hole is indicated by an open circle and is trapped at the surface, and the electron, indicated by a filled circle, can diffuse into the bulk.

smaller bandgap than bulk rutile TiO_2. For a more accurate determination of the filled states of the new TiO_2 structure and to obtain information on the electronic states making up the valence band, we performed UPS studies using synchrotron radiation.

Figure 3a,b shows valence band photoemission spectra of the TiO_2 sample. The valence band maximum (VBM) of the pristine surface occurs at 3.0 eV, which is consistent with the E_F being located close to the bottom of the conduction band. After formation of the new surface structure, a new state within the bulk bandgap of TiO_2 is observed, with a maximum at 2.1 eV below E_F, as shown in Fig. 3a,b (red curve). From comparison with STS measurements, these filled states were assigned to the new surface phase of TiO_2. It is worth noting that, although we cannot directly probe the area covered by this new surface structure in the UPS apparatus, we know from separate STM measurements on the same sample that the new structure normally covers only ~10–60% of the surface. Thus, the intensity observed in UPS would be stronger for a completely covered surface. The formation of the new structure moves the VBM of the bulk states towards E_F by ~0.3 eV. This effect is explained by band bending induced by charge transfer at the surface. As pointed out above, annealing the sample to above 800 K results in re-formation of the original TiO_2(011)–(2 × 1) surface structure. Consequently its electronic valence band structure is also regained on high-temperature annealing (Fig. 3a), demonstrating the reversibility of the structural and electronic surface transformation.

Surface electronic structure. The valence band of bulk TiO_2 is mainly composed of O 2*p* states, with some Ti 3*d* and Ti 4*sp* character acquired through hybridization with the empty Ti 3*d*/4*sp* conduction band states. Of the three main bands in the valence band, the low binding energy state (~5.5 eV) is assigned to O 2*p*–Ti 4*sp* π bonding, and the electronic band at high binding energy (~8.0 eV) is predominantly due to O 2*p*–Ti 3*d* σ bonding. The intermediate state is ascribed to an 'overlap' state[19,20]. In addition, defect bandgap states are often observed at ~0.7 eV below E_F for TiO_2(110)[21]. These states are associated with filled Ti 3*d* states in the presence of oxygen vacancies or surface hydroxyl groups that donate electrons to the Ti 3*d* states. Thus the character of the hybridization of the predominantly O 2*p* valence band with Ti states gives important indications for the bonding in TiO_2. The same electronic characteristics for the new phase as for the common rutile and anatase TiO_2 would demonstrate similar bonding. Here we used resonant photoemission spectroscopy (see Methods) to find the crucial information on the hybridization of the electronic states in the valence band of the new TiO_2 phase.

In Fig. 4a, the valence band photoemission intensity (normalized by the photon flux) is plotted for different photon energies, and Fig. 4b shows the intensity variation of the state at a binding energy of 2.1 eV, as a function of photon energy. The peak intensity jumps at $h\nu = 55$ eV, that is, at an energy that is consistent with a Ti 3*p* → Ti 4*sp* excitation. Furthermore, the variation of the peak intensity with photon energy can be described by a Fano line shape[22], as expected for this resonance behaviour. Indeed, the Fano line shape observed is clearer than normal for solid-state materials, as shown in Fig. 4b. This may be a consequence of the low-dimensional nature of this surface phase causing a stronger localization of the excited state. Thus, from resonant photoemission, we unambiguously show that the valence band maximum of this new TiO_2 phase has significant Ti 4*sp* character like other known TiO_2 phases. Consequently, we can exclude that the bandgap states are related to O vacancies or titanium sub-oxides, such as Ti_2O_3, which both exhibit mainly Ti *3d* character at the highest occupied levels[23,24]. Also, X-ray photoemission spectroscopy (XPS) taken in a separate chamber (Fig. 3c) does not show the presence of any sub-oxides at the surface; that is, the charge state of the Ti atoms at the surface is Ti^{4+} for the new structure.

Based on the experimental results, the electronic structure energy diagram for this new surface phase can be drawn as shown in Fig. 3d. The new electronic state penetrates into the bulk bandgap and reduces the surface bandgap by 0.9 eV, pushing it into the visible light spectrum. Additionally, an upward band bending at the surface is observed for our bulk samples. This energy diagram shows that visible light excitations of electron–hole pairs are possible in the surface layer. The low binding energy state in the new surface phase of TiO_2 traps holes, making them available for transfer to adsorbed molecules, while photo-excited electrons may diffuse into the bulk and can be scavenged at other surfaces not covered by the new surface structure.

Conclusions

A new narrow bandgap phase of TiO_2 has been synthesized at the surface of rutile TiO_2(011). Attempts have been made before to

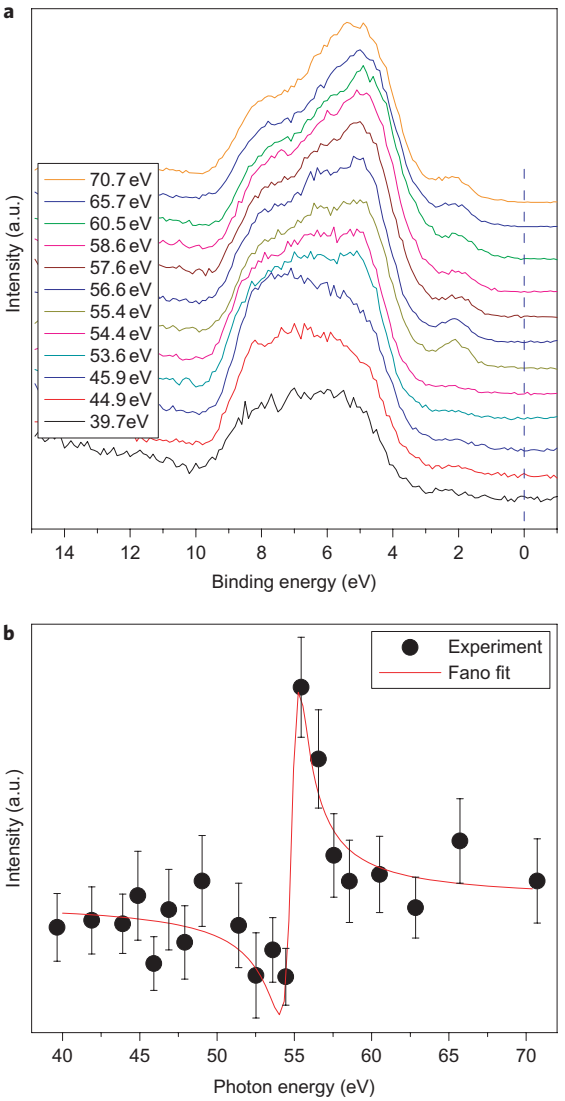

Figure 4 | Resonant photoemission measurement for the valence band maximum of the new TiO_2 phase. a, Valence band spectra acquired at different photon energies. **b**, Variation of photoemission intensity at 2.1 eV as a function of photon energy; error bars represent the standard deviation of the data. The full red line in **b** is a fit of the experimental data to a Fano line shape. The resonance at ~55 eV corresponds to Ti 4*sp* states, thus showing that the valence band maximum is due to hybridization of O 2*p* with Ti 4*sp*, indicative of a TiO_2 phase.

form new TiO_2 phases with a significantly narrowed bandgap and, therefore, visible light absorption. Notably, a high-pressure cubic phase of TiO_2 has been reported that is stable at pressures above 9 GPa (ref. 25) and exhibits visible light absorption[7]. The two-dimensional surface phase reported here bears some resemblance to the cubic form of TiO_2, in that the surface structure seen in STM images has a quasi-hexagonal structure similar to the cubic (111) plane. Although high pressures are not suitable for energy conversion applications, it is known from other materials that high-pressure phases can sometimes be stabilized as thin films or surface phases[26]. Therefore, this suggests that the current study demonstrates the existence of TiO_2 phases that can be stabilized at ambient conditions as thin films. As shown here, these phases can exhibit bandgaps tailored to the solar energy spectrum and are therefore excellent visible light absorbers. Finally, it is important to note that there is an advantage for the unusual preparation procedure for this new TiO_2 phase by re-oxidation of bulk titanium interstitials[15]. Because this synthesis procedure only requires annealing of slightly reduced TiO_2 in an oxygen atmosphere, this method may also be adapted to powder samples. Rutile TiO_2 crystallites exhibit (011) faces as the second most abundant termination after (110) faces[27], so this new surface phase may be grafted onto these facets to make visible light active catalysts.

Methods

All experiments were conducted under conditions of ultrahigh vacuum (UHV) in different vacuum chambers with base pressures in the low 1×10^{-10} torr regime. Commercial rutile TiO_2(011) single crystals (MTI Corporation) were used for the experiments. Sample preparation was done by standard surface science procedures, consisting of several cycles of low-energy Ar^+ ion sputtering and vacuum annealing to ~650 °C. To prepare the new surface structure, clean samples were annealed within the vacuum chamber in a 1×10^{-6} torr O_2 atmosphere. STM measurements were performed at room temperature with a tungsten tip. Empty states were probed with a bias voltage of 1.2 V. For STS, the tip was stabilized under tunnelling conditions of 1.2 V and 1.0 nA before disabling the feedback loop and ramping the bias voltage from –3 V to 2 V and recording the tunnelling current. The I–V curves were numerically differentiated to obtain dI/dV curves.

Valence band photoemission studies were performed at the 3m-TGM beamline[28] of the Center for Advanced Microstructure and Devices (CAMD) synchrotron in Baton Rouge, LA. Angle-resolved photoemission spectra were collected in normal emission with the linear polarized light incident at 45° to the surface normal. All spectra were normalized to the photon flux. The photon grating used in these measurements was optimized for a maximum photon flux at ~80 eV photon energy. Therefore, for lower photon energies the counting statistics is not as good as for photon energies close to 80 eV, and the spectra appear noisier in Fig. 4 than in Fig. 3. XPS was performed in a home-made XPS chamber (base pressure $< 5 \times 10^{-10}$ mbar) with a Resolve 120 Hemispherical Analyser. Normal emission spectra were recorded with a non-monochromatized Al K_α (1,486.7 eV) X-ray source placed at 45° with respect to the sample surface.

Resonant photoemission. In resonant photoemission[29], the photoemission intensity of electronic valence band states was measured as a function of photon energy. An increase in the photoemission intensity is observed as part of a de-excitation process of photo-excited states. Excited states are formed at photon energies that allow intra-atomic excitations from a core level into empty states above E_F. De-excitation is possible by photoemission from occupied states that have some orbital character of the excited state. Therefore, increased photoemission from valence band states at specific excitation thresholds gives a tell-tale sign of their hybridization with the photo-excited state. For TiO_2, photoemission resonances of valence states with excited Ti 3*d* or Ti 4*sp* states are commonly observed[19,20]. Photo-excitation occurs by promoting a Ti 3*p* core-level state to these empty states located above the Fermi level. Because the Ti 4*sp* states are ~8 eV higher above the Fermi level than the Ti 3*d* states, which form the bottom of the conduction band, hybridization of the predominantly O 2*p* valence band states with Ti 3*d* or Ti 4*sp* states can be distinguished. Ti 3*p* to Ti 3*d* excitations require an energy of ~46 eV, and the energy difference between Ti 3*p* and Ti 4*sp* is ~54 eV. Therefore, resonances at photon energies of ~46 eV or ~54 eV are manifestations of Ti 3*d* or Ti 4*sp* hybridization, respectively. For the resonance photoemission measurements reported in this article, the photon energy was varied between $h\nu = 40$ eV and $h\nu = 70$ eV, and full valence band spectra were acquired for each photon energy. Constant initial state curves were derived by measuring the photoemission intensity at a binding energy of 2.1 eV.

Received 25 October 2010; accepted 4 February 2011; published online 13 March 2011

References

1. Fujishima, A. & Honda, K. Electrochemical photolysis of water at a semiconductor electrode. *Nature* **238,** 37–38 (1972).
2. Fujishima, A., Zhang, X. & Tryk, D. A. TiO_2 photocatalysis and related surface phenomena. *Surf. Sci. Rep.* **63,** 515–582 (2008).
3. Choi, W., Termin, A. & Hoffmann, M. R. The role of metal ion dopants in quantum-sized TiO_2: correlation between photoreactivity and charge carrier recombination dynamics. *J. Phys. Chem.* **98,** 13669–13679 (1994).
4. Asahi, R., Morikawa, T., Ohwaki, T., Aoki, K. & Taga, Y. Visible-light photocatalysis in nitrogen-doped titanium oxides. *Science* **293,** 269–271 (2001).
5. Khan, S. U. M., Al-Shahry, M. & Ingler, W. B. Jr. Efficient photochemical water splitting by a chemically modified *n*-TiO_2. *Science* **297,** 2243–2245 (2002).
6. Kim, D. Y., Almeida, J. S. d., KoCi, L. & Ahuja, R. Dynamical stability of the hardest known oxide and the cubic solar material: TiO_2. *Appl. Phys. Lett.* **90,** 171903 (2007).
7. Mattesini, M. *et al.* Cubic TiO_2 as a potential light absorber in solar-energy conversion. *Phys. Rev. B* **70,** 115101 (2004).

8. Ariga, H. *et al.* Surface-mediated visible-light photo-oxidation on pure TiO_2(001). *J. Am. Chem. Soc.* **131,** 14670–14672 (2009).
9. Papageorgiou A. C. *et al.* Electron traps and their effect on the surface chemistry of TiO_2(110). *Proc. Natl Acad. Sci. USA* **107,** 2391–2396 (2010).
10. Diebold, U. The surface science of titanium dioxide. *Surf. Sci. Rep.* **48,** 53–229 (2003).
11. Torrelles, X. *et al.* Geometric structure of TiO_2(011)(2×1). *Phys. Rev. Lett.* **101,** 185501 (2008).
12. Gong, X.-Q. *et al.* The 2×1 reconstruction of the rutile TiO_2(011) surface: a combined density functional theory, X-ray diffraction, and scanning tunneling microscopy study. *Surf. Sci.* **603,** 138–144 (2009).
13. Li, M. *et al.* Oxygen-induced restructuring of the TiO_2(110) surface: a comprehensive study. *Surf. Sci.* **437,** 173–190 (1999).
14. Bowker, M. & Bennett, R. A. The role of Ti^{3+} interstitials in TiO_2 (110) reduction and oxidation. *J. Phys. Condens. Matter* **21,** 474224 (2009).
15. Stone, P., Bennett, R. A. & Bowker, M. Reactive re-oxidation of reduced TiO_2 (110) surfaces demonstrated by high temperature STM movies. *New J. Phys.* **1,** 8 (1999).
16. McCarty, K. F. Growth regimes of the oxygen-deficient TiO_2(110) surface exposed to oxygen. *Surf. Sci.* **543,** 185–206 (2003).
17. Dulub, O., Valentin, C. D., Selloni, A. & Diebold, U. Structure, defects, and impurities at the rutile TiO_2(011)–(2×1) surface: a scanning tunneling microscopy study. *Surf. Sci.* **600,** 4407–4417 (2006).
18. Batzill, M., Katsiev, K., Gaspar, D. J. & Diebold, U. Variations of the local electronic surface properties of TiO_2(110) induced by intrinsic and extrinsic defects. *Phys. Rev. B* **66,** 235401 (2002).
19. Thomas, A. G. *et al.* Comparison of the electronic structure of anatase and rutile TiO_2 single-crystal surfaces using resonant photoemission and X-ray absorption spectroscopy. *Phys. Rev. B* **75,** 035105 (2007).
20. Zhang, Z., Jeng, S.-P. & Henrich, V. E. Cation–ligand hybridization for stoichiometric and reduced TiO_2 (110) surfaces determined by resonant photoemission. *Phys. Rev. B* **43,** 12004–12011 (1991).
21. Henrich, V. E., Dresselhaus, G. & Zeiger, H. J. Observation of two-dimensional phases associated with defect states on the surface of TiO_2. *Phys. Rev. Lett.* **36,** 1335–1338 (1976).
22. Fano, U. Effects of configuration interaction on intensities and phase shifts. *Phys. Rev.* **124,** 1866–1878 (1961).
23. Smith, K. E. & Henrich, V. E. Resonant photoemission in Ti_2O_3 and V_2O_3: hybridization and localization of cation 3*d* orbitals. *Phys. Rev. B* **38,** 9571–9580 (1988).
24. Hebenstreit, E. L. D. *et al.* Sulfur on TiO_2(110) studied with resonant photoemission. *Phys. Rev. B* **64,** 115418 (2001).
25. Mattesini, M. *et al.* High-pressure and high-temperature synthesis of the cubic TiO_2 polymorph. *Phys. Rev. B* **70,** 212101 (2004).
26. Rawat, V., Zakharov, D. N., Stach, E. A. & Sands, T. D. Pseudomorphic stabilization of rocksalt GaN in TiN/GaN multilayers and superlattices. *Phys. Rev. B* **80,** 024114 (2009).
27. Ohno, T., Sarukawa, K. & Matsumura, M. Crystal faces of rutile and anatase TiO_2 particles and their roles in photocatalytic reactions. *New J. Chem.* **26,** 1167–1170 (2002).
28. Losovyj, Y. *et al.* Optimization of the 3m TGM beamline, at CAMD, for constant initial state spectroscopy. *Nucl. Instrum. Meth. A* **582,** 264–266 (2007).
29. Hüfner, S. *Photoelectron Spectroscopy: Principles and Applications* (Springer, 2003).

Acknowledgements

The photoemission data were collected at the Center for Advanced Microstructures and Devices (CAMD) in Baton Rouge, LA, operated by the Louisiana State University (LSU). The authors acknowledge financial support from the US Department of Energy, Office of Basic Energy Sciences (grant no. DE-SC0001508).

Author contributions

J.T. performed the experiments, analysed the data and wrote the paper. T.L. assisted with the experiments. M.B. directed the research and wrote the paper. All authors read and approved the contents of this manuscript.

Additional information

The authors declare no competing financial interests. Supplementary information accompanies this paper at www.nature.com/naturechemistry. Reprints and permission information is available online at http://npg.nature.com/reprintsandpermissions/. Correspondence and requests for materials should be addressed to M.B.